# Strong Metal-Support Interactions between Copper and Iron Oxide during the High Temperature Water-Gas Shift Reaction

Minghui Zhu,[#,a] Pengfei Tian,[#,a] Ravi Kurtz, [b] Thomas Lunkenbein,[c] Jing Xu,[a] Robert Schlögl,[c] Israel E. Wachs [b] and Yi-Fan Han*[,a,d]

**Abstract:** The commercial high temperature water-gas shift (HT-WGS) catalyst consists of CuO-$Cr_2O_3$-$Fe_2O_3$, where Cu functions as a chemical promoter to increase the catalytic activity but its promotion mechanism is poorly understood. In this work, a series of iron-based model catalysts were investigated with *in situ* or pseudo *in situ* characterization, steady-state WGS reaction and density function theory（DFT) calculations. For the first time, a strong metal-support interaction (SMSI) between Cu and $FeO_x$ was directly observed. During the WGS reaction, a thin $FeO_x$ overlayer migrates onto the metallic Cu particles, creating a hybrid surface structure with Cu-$FeO_x$ interfaces. The synergistic interaction between Cu and $FeO_x$ not only stabilizes the Cu clusters, but also provides new catalytic active sites that facilitate CO adsorption, $H_2O$ dissociation and WGS reaction. These new fundamental insights can potentially guide the rational design of improved iron-based HT-WGS catalysts.

The strong metal-support interaction (SMSI) was originally reported decades ago by Tauster *et al*., who found a dramatic change in the chemisorption properties of group VIII noble metals supported on $TiO_2$ after CO or $H_2$ reduction.[1] This has significantly changed the understanding of supported metal catalysts, whose morphologies were realized to dynamically evolve under reaction conditions. Under reducing environments, the oxide support can decorate the surface of metal nanoparticles to generate special contacting zones with enhanced catalytic properties.[2] The strong interaction can also improve the dispersion of metals on certain oxides that results in increased metal surface coverage or decreased particle size.[2–4]

Since then, the SMSI effect has been extensively studied and became essential for the rational design of metal-based catalysts for a variety of reactions including, but not limited to, the water-gas shift (WGS) reaction,[5,6] methanol synthesis,[7–9] CO oxidation,[10,11] $CO_2$ hydrogenation,[12] methane reforming,[13,14] oxygen reduction reaction (ORR),[15] etc. For example, Fu *et al*. developed a new class of LT-WGS catalysts with Au or Pt supported on cerium oxide. The catalytic active sites were proposed to be nonmetallic gold or platinum species strongly associated with surface cerium oxides.[16] Subsequently, Rodriguez *et al*. demonstrated by investigating the inverse $CeO_2$/Au and $TiO_2$/Au model compounds that oxide-metal interface directly participated in the LT-WGS reaction. The oxides were thought to assist water dissociation and the metals to be the catalytic active sites for CO adsorption.[5]

Besides, the SMSI effect has now also been extended to non-precious metals such as Cu. Behrens *et al*. studied the industrial Cu/ZnO/$Al_2O_3$ catalyst for methanol synthesis and observed with transmission electron microscopy (TEM) that the catalytic active sites were Cu steps decorated with oxidized Zn atoms.[9] Metastable “graphite-like” ZnO layers on the top of Cu were found to be present during reductive activation, which were proposed to be a pre-requisite for the high activity of this catalytic system.[7]

Cu also played an essential role in the industrial CuO-$Cr_2O_3$-$Fe_2O_3$ catalyst for HT-WGS reaction. In contrast to Cr that only acts as a textural promoter,[17–21] Cu was found to present in its metallic form and increase the turnover frequency (TOF) of iron-based catalysts for HT-WGS.[22–25] In turn, $FeO_x$ was reported to retard the sintering of metallic Cu nanoparticles during the reaction.[26,27] The fundamental aspects of these interactions regarding the synergistic interaction between Cu and $FeO_x$ during the HT-WGS reaction, however, are still unclear. In particular, the surface morphologies and cooperative roles of each component during the reaction were never addressed. In this work, model supported CuO/$Fe_2O_3$, $Fe_2O_3$/CuO and CuO-$Fe_2O_3$/$SiO_2$ catalysts were synthesized with the resulting surface morphologies and structure-activity relationships thoroughly examined with *in situ* characterizations, temperature-programed analysis and DFT calculations. This work, *for the first time*, provides direct evidences for SMSI between the metallic Cu clusters and iron oxide support.

The supported CuO/$Fe_2O_3$ (loading: 3 wt.%) catalyst was prepared with an incipient-wetness impregnation method. *In situ* Raman spectroscopy reveals that both the $Fe_2O_3$ support and the supported CuO/$Fe_2O_3$ catalysts possess the hematite phase (α-$Fe_2O_3$) under oxidizing dehydrated conditions (Figure 1a). Raman bands for CuO were not observed, most likely being related to the low copper content. Under reaction conditions, the hematite phase was partially reduced and transformed into the magnetite ($Fe_3O_4$) (Figure 1a), which is widely accepted as the bulk phase present for both the WGS and RWGS reactions.[28–30] The catalytic activities of the supported CuO/$Fe_2O_3$ catalyst were consistently higher than $Fe_2O_3$ at all reaction temperatures (Figure 1b). At 330°C, addition of Cu resulted in a 4-fold increase in the WGS reaction rate. As the surface areas of both catalysts were comparable after the WGS reaction ($Fe_2O_3$: 24

[a] Prof. Minghui Zhu, Dr. Pengfei Tian, Prof. Jing Xu, Prof. Yi-Fan Han
State Key Laboratory of Chemical Engineering, East China University of Science and Technology, Shanghai 200237, China
E-mail: yifanhan@ecust.edu.cn
[b] Ravi Kurtz, Prof. Israel E. Wachs
Operando Molecular Spectroscopy & Catalysis Laboratory, Department of Chemical and Biomolecular Engineering, Lehigh University, Bethlehem, Pennsylvania 18015, United States
[c] Prof. Thomas Lunkenbein, Prof. Robert Schlögl
Department of Inorganic Chemistry, Fritz-Haber-Institut der Max-Planck-Gesellschaft, Faradayweg 4-6, 14195 Berlin, Germany
[d] Prof. Yi-Fan Han
Research Center of Heterogeneous Catalysis and Engineering Sciences, School of Chemical Engineering and Energy, Zhengzhou University, Zhengzhou 450001, China
# These authors contributed equally

Supporting information for this article is given via a link at the end of the document.

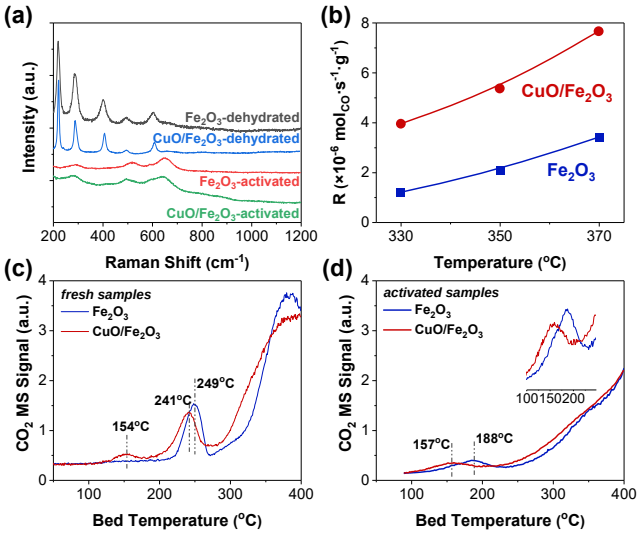


**Figure 1.** (a) *in situ* Raman spectra of $Fe_2O_3$ and $CuO/Fe_2O_3$ under dehydrated (10%$O_2$/Ar, 350°C) and RWGS conditions (5%$CO_2$/5%$H_2$/Ar, 350°C), respectively. (b) HT-WGS activity results at various temperatures (2.5%CO/2.5%$H_2O$/He). The $CO_2$ MS signal during CO-TPR over (c) fresh and (d) activated catalysts.

$m^2/g$, $CuO/Fe_2O_3$: 28 $m^2/g$), the enhancement of activity is not related to different surface areas.

The promotional effect of Cu is also apparent from CO-TPR measurements. For the fresh $Fe_2O_3$, a peak at 249°C occurs that corresponds to the bulk $Fe_2O_3 \rightarrow Fe_3O_4$ reduction (Figure 1c). Addition of Cu results in a new peak at 154°C that is assigned to $Cu^{2+} \rightarrow Cu^0$ reduction and the reduction of $Fe_2O_3$ slightly shifts to a lower temperature (249→241°C).[31–33] After activation under WGS reaction conditions, the catalyst dramatically reconstructs with formation of bulk metallic Cu and $Fe_3O_4$.[23] The CO-TPR of the activated $Fe_3O_4$ catalyst exhibits a peak at 188°C that represents the reduction of surface oxide species (Figure 1d). For the $Cu/Fe_2O_3$ catalyst, the reduction peak down-shifts to 157°C, reflecting the promotion of surface reduction by the presence of the metallic $Cu^0$ nanoparticles.[23]

To better visualize the morphological interactions between Cu and $FeO_x$, model supported $CuO\text{-}Fe_2O_3/SiO_2$ catalysts were synthesized in order to more easily monitor both phases. The TEM/STEM images and the corresponding EDX maps of the calcined catalysts revealed large particles (~60 nm) containing both Fe and Cu (Figure 2a-b). A few regions with excess amount of Cu could also be observed. This demonstrated the co-existence of intimate $CuO\text{-}Fe_2O_3$ phases as well as discrete CuO nanoparticles, which could be further confirmed by XANES analysis (Figure S1-2). The catalyst was then activated by performing the RWGS reaction and then transferred to the TEM analysis chamber in vacuum without exposure to ambient air. Metallic Cu could be observed in the activated sample with Fe species in close proximity (Figure S3-4), which demonstrated an interaction between these two components. Notably, a thin overlayer with the thickness of ~0.3 nm was observed on top of the metallic Cu (Figure 2c-d, Figure S5). In some spots, this species built up and formed small clusters with sizes below 5 nm. Unfortunately, elemental analysis under high-magnification was not applicable due to severe sample charging and drifting of the activated catalyst.

High sensitivity-low energy ion scattering (HS-LEIS) spectroscopy was then utilized to further unveil the nature of this overlayer. With 5 keV $Ne^+$ as the probe ion and 1 keV $Ar^+$ as the sputter-etching ion, the elemental distributions of Cu in the outermost surface layers could be precisely identified. Cu signals of the fresh calcined catalysts sharply increased up to a depth of 0.5 monolayer (0.5 ML), which was attributed to the residual adsorbates on the catalyst surface (Figure 2e, Figure S6).[34] After the residual adsorbates were removed by sputtering, the Cu HS-LEIS signals leveled off and remained constant beyond the first atomic layer (0.5-1.5 ML) of the catalyst. The depth-dependent analysis was extended to the activated catalysts that were pretreated by the RWGS reaction conditions and transferred to the analysis chamber under a vacuum environment (see supporting information). While surface adsorbates were still present in the outermost 0.5 ML, the Cu HS-LEIS signal for $CuO/SiO_2$ remained constant over the first atomic layer (0.5-1.5 ML) of the catalyst (Figure 2f, Figure S7). This indicated that the surface of metallic Cu nanoparticles for the activated $CuO/SiO_2$ catalyst was well exposed during the RWGS reaction. In contrast, the Cu signal for the activated

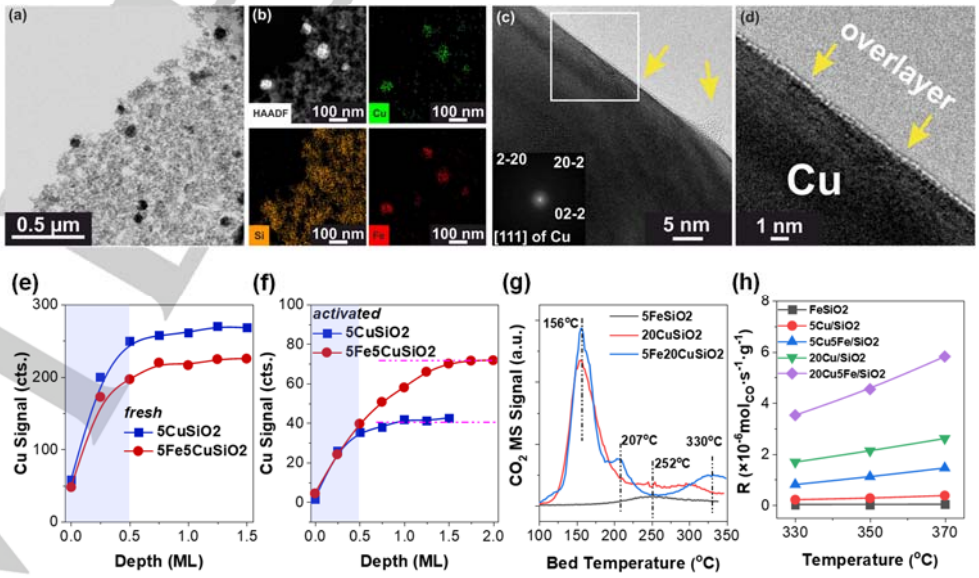


**Figure 2.** (a) TEM image of freshly calcined $5Cu5FeSiO_2$. (b) STEM images of freshly calcined $5Cu5FeSiO_2$ and the corresponding EDX mapping of Cu, Fe, O and Si. (c) TEM image of activated $20Cu5FeSiO_2$ showing a monolayer on top of metallic Cu. (d) A zoomed in region of (c). HS-LEIS depth profiles of the Cu signal for (e) freshly calcined and (f) activated $5CuSiO_2$ and $5Fe5CuSiO_2$, respectively. (g) $CO_2$ formation from CO-TPR of fresh $5FeSiO_2$, $20CuSiO_2$ and $5Fe20CuSiO_2$. (h) HT-WGS activity for all prepared supported catalysts at various temperatures (2.5%CO/2.5%$H_2O$/He).

$Fe_2O_3$-CuO/$SiO_2$ catalyst continuously increased up to a sputtered depth of 1.5 ML (Figure 2f, Figure S8). This trend, together with the TEM images, confirms the formation of a thin overlayer on the top of metallic Cu nanoparticles during the RWGS reaction. Since this oxide overlayer only existed when $Fe_2O_3$ was added, a surface $FeO_x$ monolayer is ascribed to be present. The final Cu signal intensity from the HS-LEIS spectrum for $Fe_2O_3$-CuO/$SiO_2$ was approximately 1.7 times higher than that of CuO/$SiO_2$, which reflects the improved dispersion and stabilization effect of Cu nanoparticles by $FeO_x$. The surface $FeO_x$ overlayer most probably changes the surface energy of Cu nanoparticles and suppresses their sintering.

Similar to the CuO/$Fe_2O_3$ catalyst, a facilitated CO reduction was observed on CuO-$Fe_2O_3$/$SiO_2$. Upon the addition of Cu, $T_p$ for $Fe_2O_3$ partial reduction shifted from 252°C to 207°C and the reduction of $Fe_3O_4$ was shifted from >350°C to 330°C (Figure 2g). The steady-state WGS reaction rate for CuO/$SiO_2$ was an order of magnitude higher than that of $Fe_2O_3$/$SiO_2$. Importantly, CuO-$Fe_2O_3$/$SiO_2$ exhibited a 4-fold increase in the activity against the sum of the reaction rates of $Fe_2O_3$/$SiO_2$ and CuO/$SiO_2$ (Figure 2h). The surface area of the exposed Cu sites in the activated catalysts was determined by the $N_2O$-assisted oxygen titration method.[35] The addition of $Fe_2O_3$ was found to only increase the Cu surface area by a factor of ~1.5 (30 $m^2$/g *vs.* 21 $m^2$/g), which indicates that the 4-times higher activity increasement arises from Cu-$FeO_x$ interactions at the interfaces of these two components in the activated catalysts.

To obtain additional insights about the role of $FeO_x$ at the Cu-$FeO_x$ interface during the WGS reaction, a model catalyst was synthesized by impregnating 3 wt.% $Fe_2O_3$ onto Cu nanoparticles. For the fresh catalyst, both Cu-enriched and Fe-enriched particles could be observed with TEM/STEM (Figures 3a-b). *In situ* x-ray absorption spectroscopy (XAS) was performed to investigate the electronic status of the Cu component. Both Fe-free Cu and supported $Fe_2O_3$/Cu contained fully oxidized CuO under the dehydrated conditions and were reduced to metallic Cu during the WGS reaction (Figure 3c). Subsequently, the activated catalysts were exposed to 2.5 vol.% $H_2O$/He at 350°C for 10 min in order to evaluate the capability of the catalysts for $H_2O$ dissociation. The kinetics for splitting $H_2O$ was limited on metallic Cu, which is evidenced by the negligible changes in both the x-ray absorption near edge structure (XANES) and extended x-ray absorption fine structure (EXAFS) features for Cu. In contrast, the Cu K-edge for supported $Fe_2O_3$/CuO slightly shifted to higher energy and the white line concomitantly increased after the $H_2O$ treatment that clearly reflects partial oxidation of metallic Cu. The change of the Cu oxidation state was also confirmed by observation of weak Cu-O bond features next to the dominating Cu-Cu peak from the metallic Cu component (Figure 3e). At the same time, the Fe component in $Fe_2O_3$/CuO were also partially oxidized (Figure 3f). The oxidation of Cu after the $H_2O$ treatment reflects a catalyst's ability to dissociate $H_2O$. This is the first time that facilitated $H_2O$ dissociation on Cu by $FeO_x$ species was directly demonstrated, which most likely takes place at the Cu-$FeO_x$ interfaces.

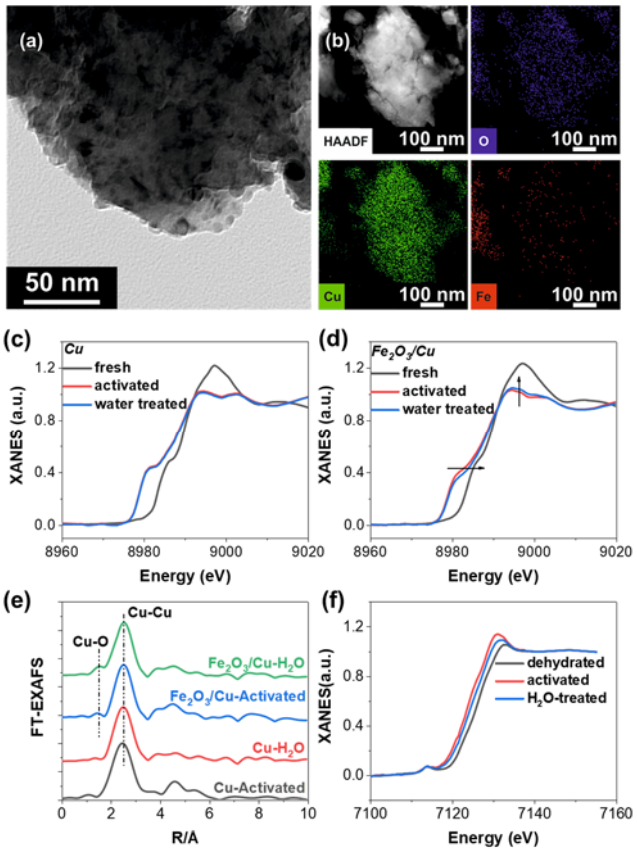


**Figure 3.** (a) TEM image of freshly calcined supported $Fe_2O_3$/CuO. (b) STEM images of freshly calcined supported $Fe_2O_3$/CuO and the corresponding EDX mapping of Cu, Fe and O. *In situ* XANES spectra of Cu K-edge for (c) Cu and (d) $Fe_2O_3$/Cu under different environmental conditions. (e) Fourier transformed EXAFS data for Cu and supported $Fe_2O_3$/Cu. (f) *in situ* XANES spectrum of Fe K-edge for supported $Fe_2O_3$/Cu under different environmental conditions.

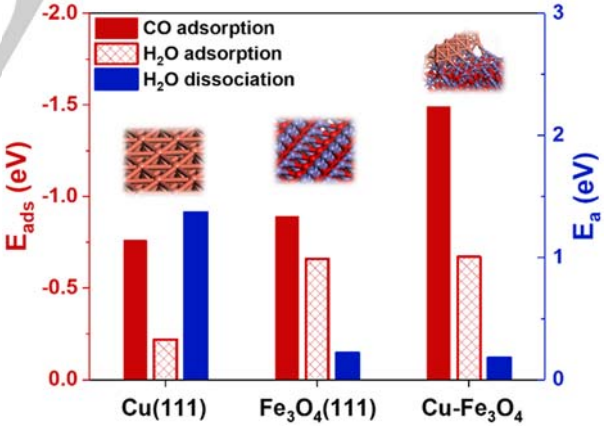


**Figure 4.** Adsorption energy of CO/$H_2O$ and activation energy for $H_2O$ dissociation on Cu (111), $Fe_3O_4$ (111) and Cu-$Fe_3O_4$ (111) interface.

DFT calculations were also performed to mechanistically interpret how the strong metal-support interaction contributes to the WGS reaction. The reaction pathways on Cu and $Fe_3O_4$ have been extensively studied, two different mechanisms were proposed (i.e. redox and associative mechanism, see SI) without reaching a consensus.[36–40] Herein, we did not seek to clarify all the elementary steps, but focused on CO adsorption, $H_2O$

adsorption and $H_2O$ dissociation, which are three common steps for both mechanisms and considered to be essential for the WGS reaction.[38] These steps were modeled on Cu (111), $Fe_3O_4$ (111) and Cu-$FeO_x$ interface with a 10-atom Cu cluster supported on the (111) surface of an $Fe_3O_4$ slab. The adsorption energy of CO on Cu (111) and $Fe_3O_4$ (111) surfaces were found to be -0.76 eV and -0.89 eV, respectively, that are close to reported values in the literature.[37,38] The strongest adsorption of CO, however, was observed at the Cu-$FeO_x$ interface (-1.49 eV). In agreement with the *in situ* XAS results, $H_2O$ dissociation was much more favored on the Cu-$FeO_x$ interface ($E_{ads}$= -0.67 eV, $E_a$=0.18 eV) than pure Cu ($E_{ads}$= -0.22 eV, $E_a$=1.37 eV). Such processes were also found to be facile on the pure $Fe_3O_4$ (111) surface ($E_{ads}$= -0.66 eV, $E_a$=0.20 eV) because of the existence of oxygen vacancies. The cooperative interaction between Cu and $FeO_x$ at the interface, thus, slightly facilitates the $H_2O$ dissociation process.

In conclusion, the SMSI effect between Cu and $FeO_x$ species has been elucidated by investigating a series of model iron oxide-based catalysts. TEM and HS-LEIS analysis of the supported CuO-$Fe_2O_3$/$SiO_2$ catalyst discovered the presence of an $FeO_x$ overlayer covering the metallic Cu nanoparticles during the HT-WGS reaction. Study of the CuO-modified $Fe_2O_3$ catalyst revealed enhanced CO reduction, and the inverse $Fe_2O_3$-doped Cu catalyst confirmed facilitation of $H_2O$ dissociation by the Cu-$FeO_x$ interface. DFT calculations further supported the synergistic interaction between Cu and $FeO_x$. Thus, Cu clusters are stabilized by $FeO_x$ and new catalytic active sites were produced that were more reactive than the individual Cu and $FeO_x$ catalysts. These findings provide new fundamental insights into commercial iron oxide-based HT-WGS catalysts to assist future efforts to increasing both activity and stability of highly active Cu-$FeO_x$ interfaces. Furthermore, the strong interaction between metallic Cu and Fe oxides may also be extended to other catalytic applications (e.g. hydrogenation reactions).

## Acknowledgements

This work was sponsored by the Program for Professor of Special Appointment (Eastern Scholar) at Shanghai Institutions of Higher Learning, Shanghai Sailing Program (19YF1410600) and the Fundamental Research Funds for the Central Universities (222201718002). P.T acknowledges the support from National Natural Science Foundation of China (No. 21808057). I.E.W. and R.K. acknowledge the financial support from National Science Foundation Grant CBET-1511689. We thank Prof. Anatoly Frenkel for collaborating with us on the XAS measurements and analysis. Beamline X18A of the NSLS is supported in part by the U.S. DOE Grant No. DE-FG02-05ER15688. The NSLS is supported by U.S. DOE Contract No. DE-AC02-98CH10886. Dr. Henry Luftman is thanked for assisting with the collection of the HS- LEIS data. We appreciate the generous help in XAS experiments from the staff of the BL14W1 beamline at the Shanghai Synchrotron Radiation Facility (SSRF).

**Keywords:** strong metal-support interaction • water-gas shift reaction • hydrogen • copper • iron oxide

[1] S. J. Tauster, S. C. Fung, R. L. Garten, *J. Am. Chem. Soc.* **1978**, *100*, 170–175.

[2] S. J. Tauster, *Acc. Chem. Res.* **1987**, *20*, 389–394.

[3] J. J. Liu, *ChemCatChem* **2011**, *3*, 934–948.

[4] S. Bernal, J. . Calvino, M. . Cauqui, J. . Gatica, C. Larese, J. . Pérez Omil, J. . Pintado, *Catal. Today* **1999**, *50*, 175–206.

[5] J. A. Rodriguez, S. Ma, P. Liu, J. Hrbek, J. Evans, M. Perez, *Science* **2007**, *318*, 1757–1760.

[6] J. A. Rodriguez, P. Liu, J. Hrbek, J. Evans, M. Pérez, *Angew. Chemie Int. Ed.* **2007**, *46*, 1329–1332.

[7] T. Lunkenbein, J. Schumann, M. Behrens, R. Schlögl, M. G. Willinger, *Angew. Chemie Int. Ed.* **2015**, *54*, 4544–4548.

[8] J. Graciani, K. Mudiyanselage, F. Xu, A. E. Baber, J. Evans, S. D. Senanayake, D. J. Stacchiola, P. Liu, J. Hrbek, J. F. Sanz, et al., *Science* **2014**, *345*, 546–550.

[9] M. Behrens, F. Studt, I. Kasatkin, S. Kuhl, M. Havecker, F. Abild-Pedersen, S. Zander, F. Girgsdies, P. Kurr, B.-L. Kniep, et al., *Science* **2012**, *336*, 893–897.

[10] X. Liu, M.-H. Liu, Y.-C. Luo, C.-Y. Mou, S. D. Lin, H. Cheng, J.-M. Chen, J.-F. Lee, T.-S. Lin, *J. Am. Chem. Soc.* **2012**, *134*, 10251–10258.

[11] A. S. Ivanova, E. M. Slavinskaya, R. V. Gulyaev, V. I. Zaikovskii, O. A. Stonkus, I. G. Danilova, L. M. Plyasova, I. A. Polukhina, A. I. Boronin, *Appl. Catal. B Environ.* **2010**, *97*, 57–71.

[12] S. Li, Y. Xu, Y. Chen, W. Li, L. Lin, M. Li, Y. Deng, X. Wang, B. Ge, C. Yang, et al., *Angew. Chemie Int. Ed.* **2017**, *56*, 10761–10765.

[13] D. Liu, X. Y. Quek, W. N. E. Cheo, R. Lau, A. Borgna, Y. Yang, *J. Catal.* **2009**, *266*, 380–390.

[14] Z. Liu, D. C. Grinter, P. G. Lustemberg, T.-D. Nguyen-Phan, Y. Zhou, S. Luo, I. Waluyo, E. J. Crumlin, D. J. Stacchiola, J. Zhou, et al., *Angew. Chemie Int. Ed.* **2016**, *55*, 7455–7459.

[15] A. Lewera, L. Timperman, A. Roguska, N. Alonso-Vante, *J. Phys. Chem. C* **2011**, *115*, 20153–20159.

[16] Q. Fu, H. Saltsburg, M. Flytzani-Stephanopoulos, *Science* **2003**, *301*, 935–938.

[17] F. Meshkani, M. Rezaei, *J. Ind. Eng. Chem.* **2014**, *20*, 3297–3302.

[18] F. Meshkani, M. Rezaei, M. H. Aboonasr Shiraz, *Chem. Eng. Res. Des.* **2016**, *113*, 9–16.

[19] F. Meshkani, M. Rezaei, *Chem. Eng. Res. Des.* **2015**, *95*, 288–297.

[20] F. Meshkani, M. Rezaei, *Chem. Eng. J.* **2015**, *260*, 107–116.

[21] D. Devaiah, P. G. Smirniotis, *Ind. Eng. Chem. Res.* **2017**, *56*, 1772–1781.

[22] M. Zhu, I. E. Wachs, *ACS Catal.* **2016**, *6*, 1764–1767.

[23] M. Zhu, T. C. R. Rocha, T. Lunkenbein, A. Knop-Gericke, R. Schlögl, I. E. Wachs, *ACS Catal.* **2016**, *6*, 4455–4464.

[24] M. Estrella, L. Barrio, G. Zhou, X. Wang, Q. Wang, W. Wen, J. C. Hanson, A. I. Frenkel, J. A. Rodriguez, *J. Phys. Chem. C* **2009**, *113*, 14411–14417.

[25] A. Jha, D.-W. Jeong, J.-O. Shim, W.-J. Jang, Y.-L. Lee, C. V. Rode, H.-S. Roh, *Catal. Sci. Technol.* **2015**, *5*, 2752–2760.

[26] H. Yan, X.-T. Qin, Y. Yin, Y.-F. Teng, Z. Jin, C.-J. Jia, *Appl. Catal. B Environ.* **2018**, *226*, 182–193.

[27] C. S. Chen, W. H. Cheng, S. S. Lin, *Appl. Catal. A Gen.* **2004**, *257*, 97–106.
[28] M. Zhu, I. E. Wachs, *ACS Catal.* **2016**, *6*, 722–732.
[29] C. Rhodes, G. J. Hutchings, A. M. Ward, *Catal. Today* **1995**, *23*, 43–58.
[30] M. Zhu, I. E. Wachs, *Catal. Today* **2018**, *311*, 2–7.
[31] D.-W. Jeong, A. Jha, W.-J. Jang, W.-B. Han, H.-S. Roh, *Chem. Eng. J.* **2015**, *265*, 100–109.
[32] G. K. Reddy, K. Gunasekera, P. Boolchand, J. Dong, P. G. Smirniotis, *J. Phys. Chem. C* **2011**, *115*, 7586–7595.
[33] V. Subramanian, E. S. Gnanakumar, D.-W. Jeong, W.-B. Han, C. S. Gopinath, H.-S. Roh, *Chem. Commun.* **2013**, *49*, 11257.
[34] W. P. A. Jansen, J. Beckers, J. C. v. d. Heuvel, A. W. D. v. d. Gon, A. Bliek, H. H. Brongersma, *J. Catal.* **2002**, *210*, 229–236.
[35] C. J. G. V. Der Grift, A.F.H.Wielers, B.P.J.Jogh, J. V. Beunum, M. D. Boer, M.Versluijs-Helder, J.W.Geus, *J. Catal.* **1991**, *131*, 178–189.
[36] P. Xue, Z. Fu, Z. Yang, *Phys. Lett. A* **2015**, *379*, 607–612.
[37] Y.-X. Wang, G.-C. Wang, *ACS Catal.* **2019**, 2261–2274.
[38] L. Huang, B. Han, Q. Zhang, M. Fan, H. Cheng, *J. Phys. Chem. C* **2015**, *119*, 28934–28945.
[39] M. Zhu, I. E. Wachs, *ACS Catal.* **2016**, *6*, 2827–2830.
[40] G. K. Reddy, P. Boolchand, P. G. Smirniotis, *J. Phys. Chem. C* **2012**, *116*, 11019–11031.

## Entry for the Table of Contents

# COMMUNICATION

**Strong metal-support interaction** between metallic copper and iron oxides were observed during the HT-WGS reaction. Such synergistic interaction not only stabilizes the Cu clusters, but also provides new catalytic active sites that facilitate CO adsorption, $H_2O$ dissociation and WGS reaction.

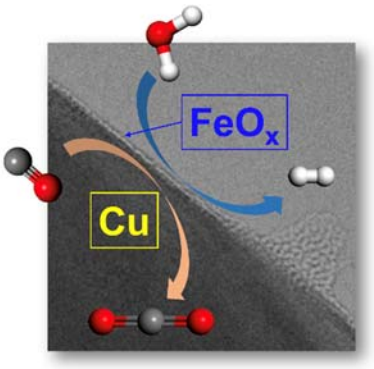


*Minghui Zhu, Pengfei Tian, Ravi Kurtz, Thomas Lunkenbein, Jing Xu, Robert Schlögl, Israel E. Wachs and Yi-Fan Han*

***Page No. – Page No.***

**Strong Metal-Support Interactions between Copper and Iron Oxide during the High Temperature Water-Gas Shift Reaction**